University of Groningen

The LysR-type transcriptional regulator CbbR controlling autotrophic CO2 fixation by Xanthobacter flavus is an NADPH sensor

van Keulen, G; Girbal, L; van den Bergh, E.R E; Dijkhuizen, L.; Meijer, W.G

Published in:
Journal of Bacteriology

Publication date:
1998

[Link to publication in University of Groningen/UMCG research database](#)

Citation for published version (APA):
van Keulen, G., Girbal, L., van den Bergh, E. R. E., Dijkhuizen, L., & Meijer, W. G. (1998). The LysR-type transcriptional regulator CbbR controlling autotrophic CO2 fixation by Xanthobacter flavus is an NADPH sensor. *Journal of Bacteriology*, *180*(6), 1411-1417.

The LysR-Type Transcriptional Regulator CbbR Controlling Autotrophic CO$_2$ Fixation by *Xanthobacter flavus* Is an NADPH Sensor

G. VAN KEULEN, L. GIRBAL, E. R. E. VAN DEN BERGH, L. DIJKHUIZEN, AND W. G. MEIJER*

*Department of Microbiology, Groningen Biomolecular Sciences and Biotechnology Institute,
University of Groningen, 9751 NN Haren, The Netherlands*

Autotrophic growth of *Xanthobacter flavus* is dependent on the fixation of carbon dioxide via the Calvin cycle and on the oxidation of simple organic and inorganic compounds to provide the cell with energy. Maximal induction of the *cbb* and *gap-pgk* operons encoding enzymes of the Calvin cycle occurs in the absence of multicarbon substrates and the presence of methanol, formate, hydrogen, or thiosulfate. The LysR-type transcriptional regulator CbbR regulates the expression of the *cbb* and *gap-pgk* operons, but it is unknown to what cellular signal CbbR responds. In order to study the effects of low-molecular-weight compounds on the DNA-binding characteristics of CbbR, the protein was expressed in *Escherichia coli* and subsequently purified to homogeneity. CbbR of *X. flavus* is a dimer of 36-kDa subunits. DNA-binding assays suggested that two CbbR molecules bind to a 51-bp DNA fragment on which two inverted repeats containing the LysR motif are located. The addition of 200 μM NADPH, but not NADH, resulted in a threefold increase in DNA binding. The apparent $K_{d_{\text{NADPH}}}$ of CbbR was determined to be 75 μM. By using circular permutated DNA fragments, it was shown that CbbR introduces a 64° bend in the DNA. The presence of NADPH in the DNA-bending assay resulted in a relaxation of the DNA bend by 9°. From the results of these in vitro experiments, we conclude that CbbR responds to NADPH. The in vivo regulation of the *cbb* and *gap-pgk* operons may therefore be regulated by the intracellular concentration of NADPH.

During autotrophic growth of *Xanthobacter flavus*, CO$_2$ is assimilated via the Calvin cycle (16, 17). The energy required to operate the Calvin cycle is provided by the oxidation of methanol, formate, thiosulfate, or hydrogen (20). To date, three unlinked transcriptional units encoding Calvin cycle enzymes have been identified: the *cbb* operon, the *gap-pgk* operon, and the *tpi* gene (18, 19, 21, 24). The key enzymes of the Calvin cycle, ribulose-1,5-bisphosphate carboxylase-oxygenase (*cbbLS*) and phosphoribulokinase, are encoded within the *cbb* operon (19, 23).

The LysR-type transcriptional regulator CbbR has been identified in several chemo- and photoautotrophic bacteria (5, 6, 13, 19, 25, 32, 37, 38, 42). This protein controls the expression of the *cbb* operon and, in *X. flavus*, also the *gap-pgk* operon (24). LysR-type proteins recognize inverted repeats containing the LysR motif (7). Two LysR motif-containing inverted repeats are present in the intergenic region between *cbbR* and *cbbL* in which the promoter of the *cbbLSXFPTAE* operon is located (37). Promoter-distal repeat IR$_1$ is a perfect repeat, whereas promoter-proximal repeat IR$_2$ is imperfect (Fig. 1).

The expression of the *cbb* and *gap-pgk* operons is maximally induced during growth in the absence of multicarbon substrates and in the presence of suitable autotrophic substrates, e.g., methanol (4, 20, 24). Although it is firmly established that CbbR plays an important role in transducing cellular signals to the transcription apparatus, the nature of these signals is still unknown. The results from studies with mutants of *X. flavus*, *Ralstonia eutropha*, and *Pseudomonas oxalaticus* blocked in gly-

colysis and isocitrate lyase indicated that the intracellular concentration of a glycolytic intermediate, e.g., phosphoenolpyruvate or acetyl coenzyme A, is an important factor in the regulation of the *cbb* operon (10, 18, 21, 22, 28). A correlation between the generation of reducing equivalents and the induction of the Calvin cycle has been demonstrated in both chemo- and photoautotrophic bacteria, suggesting that the intracellular concentration of NAD(P)H could be important in the regulation of the *cbb* operon (4, 9, 15, 29, 40). A low intracellular phosphoenolpyruvate concentration signals that insufficient carbon is available, which would necessitate CO$_2$ fixation; a high level of NADH signals that sufficient reducing power is available for the Calvin cycle to proceed. Interestingly, the activity of bacterial phosphoribulokinase is inhibited by phosphoenolpyruvate and stimulated by NADH (34).

A number of LysR-type proteins have been shown to respond to the presence of low-molecular-weight ligands by an altered affinity for their DNA-binding sites and a decrease in the DNA-bending angle introduced upon binding of the protein (31). To obtain further insight in the molecular mechanism by which CbbR regulates the transcription of the *cbb* operon, the effects of low-molecular-weight compounds on the interaction of CbbR with its cognate binding sites were investigated. This paper describes the purification of CbbR of *X. flavus* and its interaction with NADPH.

MATERIALS AND METHODS

Bacterial strains and plasmids. The bacterial strains and plasmids used in this study are listed in Table 1.

Media and growth conditions. *Escherichia coli* strains were grown on Luria-Bertani medium at 37°C (30). When appropriate, the following supplements were added: ampicillin, 100 μg/ml; 5-bromo-4-chloro-3-indolyl-β-D-galactopyranoside, 20 μg/ml; chloramphenicol, 100 μg/ml; isopropyl-β-D-thiogalactopyranoside (IPTG), 0.1 mM. Agar was added for solid medium (1.5% [wt/vol]).

DNA manipulations. Plasmid DNA was isolated via the alkaline lysis method of Birnboim and Doly (1). DNA-modifying enzymes were obtained from Boehr-

* Corresponding author. Present address: Department of Industrial Microbiology, University College Dublin, Belfield Campus, Dublin 4, Ireland. Phone: 353-1-7061512. Fax: 353-1-7061183. E-mail: wim.meijer@ucd.ie.
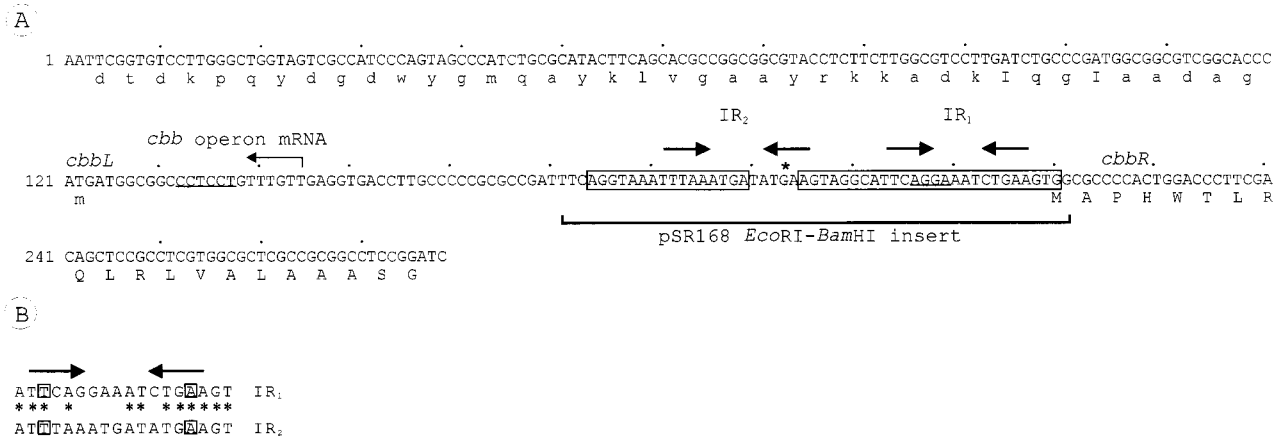
FIG. 1. (A) Nucleotide sequences of the 277- and 56-bp DNA fragments used in the band shift assays. The five nucleotides of the 56-bp fragment derived from the vector are not shown. The positions of the putative binding sites of CbbR (IR_1 and IR_2) are indicated by arrows. The translations of *cbbL* and *cbbR* are shown below the nucleotide sequence. The translation of *cbbL* is from the reverse complement (lowercase letters). Putative ribosome-binding sites are underlined. The transcriptional start site of the *cbb* operon (19) is indicated by an arrow. The nucleotides protected by CbbR from DNase I digestion are boxed, and the position of the DNase I-hypersensitive nucleotide is indicated by the asterisk. (B) Alignment of IR_1 and IR_2, the putative binding sites of CbbR. Identical nucleotides are indicated by asterisks. The nucleotides making up the LysR motif (T-N_{11}-A) are boxed.

inger and used in accordance with the manufacturer's instructions. DNA fragments were isolated from agarose gels by using the Qiaex DNA purification kit (Qiagen). Other DNA manipulations were done in accordance with standard protocols (30). Oligonucleotides were obtained from Eurogentec. PCRs were carried out by using PWO polymerase as recommended by the manufacturer (Boehringer). Dideoxy sequencing reactions of plasmid DNA were performed with modified T7 DNA polymerase (Sequenase; U.S. Biochemical Corporation) and [^{35}S]dATP as recommended by the manufacturer.

Construction of a CbbR expression vector. The 5′ end of *cbbR* was amplified from pSR1 by PCR using oligonucleotides CR1a (5′-CGCCATATGGCGCCC CACTGGACCCTTCG-3′) and CR2 (5′-CATAGGATCCGGAGGCCGCGGC GAGC-3′), containing, respectively, an *Nde*I and a *Bam*HI restriction site. The resulting DNA fragment was ligated into *Sma*I-digested pBluescript KS. The resulting plasmid was digested with *Nde*I and *Bam*HI and ligated into pET3a digested with the same enzymes. The *Sac*II-*Bam*HI fragment of pSR1 containing the 3′ end of *cbbR* was subsequently ligated into expression vector pET3a, containing the 5′ end of *cbbR*, yielding pER500. The nucleotide sequence of the 5′ end of the modified *cbbR* gene was determined to verify that unwanted mutations were not introduced in the PCR.

Expression of CbbR. *E. coli* BL21(DE3) containing pLysE and pER500 was grown in 3 liters of Luria-Bertani medium (with 50 μg of ampicillin and 100 μg of chloramphenicol per ml) at 30°C until an optical density at 663 nm of 0.5 was reached. IPTG was added to a final concentration of 1 mM, and growth was allowed to proceed for an additional 3 h. Cells were harvested via centrifugation and resuspended in ice-cold buffer A (25 mM Tris-HCl [pH 7.8], 1 mM EDTA, 1 mM dithiothreitol, 10% [vol/vol] glycerol).

Purification of CbbR. All steps were performed at 4°C, except when noted otherwise. The presence of CbbR during purification was determined by using

denaturing gel electrophoresis, in which it could be detected as the most abundant protein. DNA binding of CbbR was assayed by using a band shift assay. Cell extracts of IPTG-induced *E. coli* BL21(DE3)/pLysE/pER500 were prepared freshly by passing the cell suspension twice through a French pressure cell (1.4 × 10^5 kN/m^2) after the addition of phenylmethylsulfonyl fluoride (0.1 mM). Cell debris was removed by 30 min of centrifugation at 35,000 × *g*. The cell extract was applied to a Q Sepharose (Pharmacia) column (height, 4.5 cm; diameter, 3.5 cm) equilibrated in buffer A at a flow rate of 3 ml/min. The flowthrough fraction containing CbbR was applied to a heparin (Pharmacia) column (height, 11 cm; diameter, 2 cm) equilibrated in buffer A. The heparin column was eluted with a linear gradient of KCl in buffer A (12.5 mM/ml; flow rate, 2 ml/min). The fractions containing CbbR were pooled, and ($NH_4)_2SO_4$ was added to a final concentration of 1 M. The pooled fractions were subsequently applied to a phenyl-Superose HR5/5 column (Pharmacia) equilibrated in buffer A containing 1 M ($NH_4)_2SO_4$. CbbR was eluted with a decreasing ($NH_4)_2SO_4$ gradient (33.8 mM/ml) in buffer A, at a flow rate of 0.5 ml/min. The active fractions were pooled, desalted by using a PD10 column (Pharmacia) equilibrated with buffer A, and applied to an SP-Superose (Pharmacia) column (height, 6 cm; diameter, 1.2 cm) equilibrated in buffer B (25 mM KPO_4 [pH 6.8], 1 mM EDTA, 1 mM dithiothreitol, 10% [vol/vol] glycerol). CbbR was eluted with a linear KCl gradient (33 mM/ml).

The molecular weight (MW) of native CbbR was determined at 4°C by gel filtration with a Superdex 200 column (Pharmacia) which was calibrated with thyroglobin (MW, 670,000), gamma globulin (MW, 158,000), ovalbumin (MW, 44,000), myoglobin (MW, 17,000), and cobalamin (MW, 1,350) obtained from Bio-Rad. Protein was determined as described by Bradford, by using bovine serum albumin (BSA) as the standard (2).

TABLE 1. Bacteria and plasmids used in this study

Strain or plasmid	Genotype or characteristics	Source or reference
E. coli		
DH5α	*supE44 ΔlacU169* (φ80*lacZ*ΔM15) *hsdR17 recA1 endA1 gyrA96 thi-1 relA1*	Bethesda Research Laboratories
BL21(DE3) containing pLysE		33
Plasmids		
pTZ19U	Ap^r *lacZ′*; cloning vector	Bio-Rad
pET3a	Ap^r; T7 promoter, expression vector	33
pBluescript KS	Ap^r *lacZ′*; cloning vector	Stratagene
pBEND4	Ap^r; circular permutation vector	43
pER500	Ap^r; CbbR expression vector	This study
pSR1	Ap^r; 1.8-kb *Sma*I fragment containing *cbbR* and *cbbL′*	37
pSR168	Ap^r; 56-bp *Bam*HI-*Eco*RI fragment containing IR_1 and IR_2	This study
pLG168	Ap^r; 68-bp *Hin*dIII-*Bam*HI fragment containing IR_1 and IR_2	This study
pTZ00	Ap^r; 277-bp fragment containing *cbbR-cbbL* intergenic region	This study

Preparation of DNA fragments used in binding studies. The intergenic region between *cbbR* and *cbbL* was amplified by PCR from pSR1 by using oligonucleotides Preind (5′-CGCGAATTCGTGTCCTTGGGCTGGTAG-3′) and CR2 (5′-CATAGGGATCCGGAGGCCGCGGCGAGC-3′). The resulting 285-bp DNA fragment was ligated into pTZ19U digested with *Sma*I, yielding pTZ00. A DNA fragment containing the CbbR-binding sites without flanking DNA sequences was obtained by a PCR with pSR1 as the template and oligonucleotides Pr2 (5′-CGGGGATCCACTTCAGATTTCCT-3′) and Pr8 (5′-CTTGCCCCCGCG CCGAATTCAGG-3′). The resulting fragment was digested with *Bam*HI and *Eco*RI and subsequently cloned into pBluescript KS digested with *Bam*HI and *Eco*RI, which yielded pSR168. The nucleotide sequences of the inserts of pSR168 and pTZ00 were determined to verify that mutations were not introduced during the PCR.

Labeling of DNA fragments. To obtain DNA fragments for use in band shift assays, pTZ00 and pSR168 were digested with *Bam*HI and *Eco*RI and labeled with [α-^{32}P]dCTP in a mixture (30 μl) containing 50 ng of DNA, 100 μM dATP, 100 μM dCTP, 100 μM dTTP, 1 μCi of [α-^{32}P]dCTP, 1 U of Klenow enzyme, 10 mM Tris-HCl (pH 8.0), 5 mM MgCl$_2$, 100 mM NaCl, and 1 mM β-mercaptoethanol. Following incubation at room temperature for 30 min, 50 μM deoxynucleoside triphosphates were added and the reaction was allowed to proceed for an additional 15 min. The reaction was stopped by adding 15 mM EDTA to the mixture, and the DNA fragment was subsequently purified by using the Qiaquick PCR purification kit (Qiagen). DNA fragments with blunt ends and oligonucleotides were labeled with [γ-^{32}P]ATP (30 μCi) by using T4 polynucleotide kinase (30).

Band shift assay. Band shift assays were performed as described previously, by using [^{32}P]dCTP-labeled DNA fragments, except that 20 μg of BSA was included in the binding assay (37). Metabolites were included in the incubation mixture to a final concentration of 200 μM. The samples were subjected to nondenaturing gel electrophoresis using 6% acrylamide gels in Tris-borate buffer (30) and run at 4°C and 10 V/cm. Following drying, the gel was analyzed by autoradiography. The radioactivity in the gel was quantified with a Molecular Dynamics Phospho-Imager using the ImageQuant program, version 3.3, from the same company.

Band shift assay using circular permuted DNA fragments. The method used employs the band shift assay to examine DNA bending (43). Digestion of pSR168 with *Hin*dIII and *Bam*HI liberates a 68-bp fragment which was treated with Klenow enzyme and subsequently cloned into *Hpa*I-digested pBend4 (43), yielding pLG168. The nucleotide sequence of the insert in pLG168 was determined to confirm the correct insertion in pBend4. Plasmid pLG168 was subsequently digested with either *Bgl*II, *Nhe*I, *Xho*I, *Eco*RV, *Pvu*II, or *Sma*I, resulting in circular permutated DNA fragments of 189 bp, containing the CbbR-binding sites at various distances from the end of the molecule. Following labeling, the fragments were used in the band shift assay. The bending angles (α) were calculated by using the formula $\mu_m/\mu_e = \cos(\alpha/2)$, where μ_m and μ_e represent the gel mobilities of DNA molecules with bends in the middle and at the ends, respectively (43).

DNase I footprinting. Amplification of pTZ00 by using radiolabeled oligonucleotide M13 (-40) (5′-GTTTTCCCAGTCACGAC-3′) and unlabeled oligonucleotide M13 reverse (-48) (5′-AGCGGATAACAATTTCACACAGGA-3′) resulted in a DNA fragment of 464 bp, containing the *cbbR-cbbL* intergenic region. The PCR product was subsequently purified by using the Qiaquick PCR purification kit (Qiagen). Purified CbbR was incubated with the radiolabeled PCR product (100,000 cpm) at 30°C for 30 min in a reaction mixture (50 μl) containing 25 mM Tris-HCl, 1 mM EDTA, 0.1 mM dithiothreitol, 10% (vol/vol) glycerol, and 0.4 mg of BSA per ml. Subsequently, 10 μl of DNase I solution (1 U of DNase I [fast protein liquid chromatography pure; Pharmacia], 10 mM Tris-HCl [pH 7.5], 25 mM KCl, 10 mM CaCl$_2$, 10 mM MgCl$_2$, 10% [vol/vol] glycerol) was added. Following incubation at 21°C for 1 min, the reaction was stopped by adding 140 μl of water and 200 μl of phenol-chloroform (1:1 ratio). The aqueous layer was extracted once with chloroform, and DNA was subsequently precipitated with ethanol and dried. The DNA pellet was dissolved in gel-loading buffer (90% [vol/vol] formamide, 0.025% [wt/vol] xylene cyanol FF, 0.025% [wt/vol] bromophenol blue, Tris-borate buffer [30]); 2.5 μl of gel-loading buffer was subsequently loaded on a 6% sequencing gel (30). Each lane contained an equal amount of radioactivity. A G+A sequencing ladder was prepared as described previously (26).

RESULTS

Purification of CbbR. To facilitate purification of CbbR, an efficient expression system was constructed by replacing the GTG initiation codon of *cbbR* with ATG and by placing *cbbR* downstream from the T7 promoter present on pET3a. Following induction of T7 RNA polymerase in *E. coli* BL21(DE3)/pLysE/pER500, CbbR was present as the most abundant protein in the cell extract. CbbR was purified from *E. coli* BL21(DE3)pLysE/pER500 in four steps. The resulting CbbR preparation was homogeneous, as judged by sodium dodecyl sulfate-polyacrylamide gel electrophoresis (Fig. 2). The CbbR
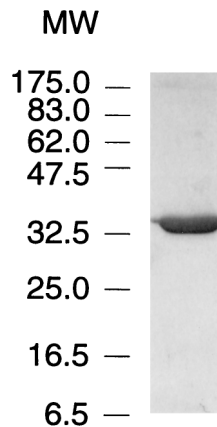

FIG. 2. Coomassie brilliant blue-stained denaturing polyacrylamide gel showing CbbR (10 μg) purified from IPTG-induced *E. coli* BL21(DE3)pLysE/pER500. The MW standards used are shown.

monomer had a molecular mass of 36 kDa, which is in close agreement with the mass (35,971 Da) predicted from the CbbR amino acid sequence (37). The molecular mass of native CbbR at 4°C, as determined by gel filtration, was estimated to be 79 kDa, indicating that CbbR of *X. flavus* is a dimer in solution. Interestingly, the protein from *R. eutropha* is a dimer at room temperature and a tetramer at 4°C (14). In contrast to CbbR from *R. eutropha*, the CbbR protein from *X. flavus* is completely soluble in buffers containing 25 mM KCl (14). Purified CbbR was stable, with virtually no loss of DNA-binding activity when stored at -80°C for 2 weeks in buffer A.

Localization of CbbR-binding sites. We previously described the binding of CbbR to two binding sites in the intergenic region between *cbbR* and *cbbL* which contains a perfect (IR$_1$) and an imperfect (IR$_2$) inverted repeat containing the LysR motif (37). To determine whether CbbR binds to a DNA fragment containing only these inverted repeats, a 56-bp *Bam*HI-*Eco*RI DNA fragment (Fig. 1) of pSR168 was radiolabeled and used in a band shift assay. Two protein-DNA complexes with high and low electrophoretic mobilities were observed, which are interpreted to be the result of the interaction between the *Bam*HI-*Eco*RI DNA fragment with one and two CbbR dimers, respectively (data not shown).

To confirm the presence of two CbbR-binding sites on the 56-bp *Bam*HI-*Eco*RI DNA fragment, a 464-bp DNA fragment containing the *cbbR-cbbL* intergenic region was end labeled and used in a DNase I footprint assay with purified CbbR (Fig. 3). CbbR protected nucleotides -75 to -29 relative to the transcriptional start site of the *cbb* operon from DNase I digestion. In the protected area, nucleotides between -75 and -50 were strongly protected, whereas protection of nucleotides between -44 and -29 was weaker. A DNase I-hypersensitive site at -48 was present between the two regions, which could be the result of DNA bending by CbbR. The results from the band shift assay and the DNase I footprint, therefore, show that CbbR binds to two sites located between positions -29 and -75 relative to the transcription initiation site of the *cbb* operon.

NADPH enhances the DNA binding of cbbR. In general, LysR-type proteins activate transcription following the binding of low-molecular-weight ligands. In addition, binding of these ligands frequently results in a modest increase or decrease in the DNA-binding affinity of this type of transcriptional regulator (31). The results from physiological studies indicate that transcription of the *cbb* operon in *X. flavus* is enhanced in the
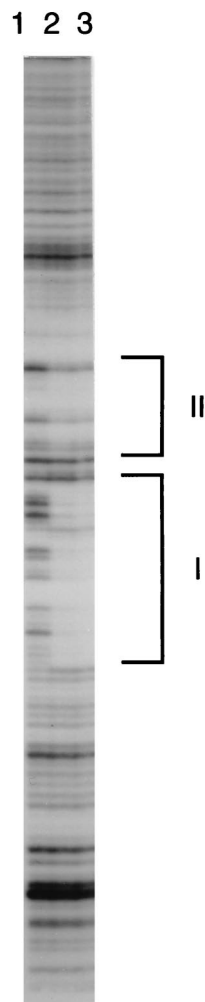
FIG. 3. DNase I footprint of a 464-bp DNA fragment containing the *cbbR-cbbL* intergenic region. The brackets indicate the positions of the strongly and weakly protected nucleotides from, respectively, −75 to −50 (I) and −44 to −29 (II). Lanes: 1, CbbR not added; 2, 0.34 μg of CbbR added; 3, 1.7 μg of CbbR added. The nucleotide sequence of the protected regions and the DNase I-hypersensitive site located between the two protected regions is shown in Fig. 1.

FIG. 4. Effects of pyridine dinucleotides (200 μM) on the DNA-binding characteristics of CbbR. A band shift assay was done with the 277-bp *Eco*RI-*Bam*HI DNA fragment (10,000 cpm) of pTZ00 and purified CbbR (27 ng of CbbR). Lanes: 1, no CbbR added; 2, CbbR; 3, CbbR plus NADPH; 4, CbbR plus NADH; 5, CbbR plus NADP; 6, CbbR plus NAD. Arrows indicate the positions of the unbound DNA and the protein-DNA complexes of low (complex 1) and high (complex 2) electrophoretic mobility.

absence of carbon sources and in the presence of methanol, formate, or hydrogen. We therefore tested whether metabolites associated with glycolysis (phosphoenolpyruvate, 2-phosphoglycerate, and 3-phosphoglycerate) or energy metabolism (ATP, ADP, NADH, NAD, NADPH, and NADP) influence the in vitro binding of purified CbbR to its cognate binding sites. The addition of 200 μM NADPH to the binding assay resulted in an increase in DNA binding, whereas the other metabolites tested did not affect DNA binding by CbbR (Fig. 4).

The addition of NADPH to the DNA-binding assay had two effects on DNA binding by CbbR (Fig. 5). The total amount of ^{32}P-labeled DNA bound to CbbR increased threefold when the NADPH concentration was increased from 0 to 500 μM. Saturation occurred at approximately 200 μM NADPH; the apparent $K_{d_{NADPH}}$ of CbbR was estimated to be 75 μM. In addition, the ratio of complex 1 to complex 2 changed dramatically. In the absence of NADPH, 65% of the ^{32}P-labeled DNA bound to CbbR was present in complex 1, representing the bi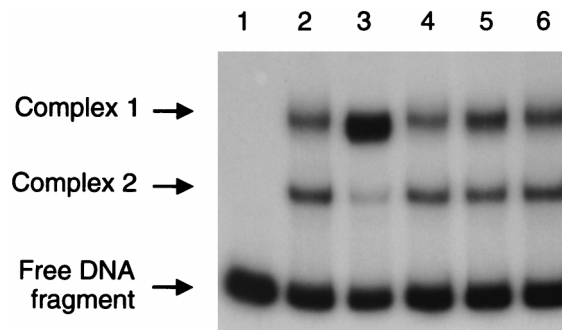nding of CbbR to both cognate binding sites. In the presence of 500 μM NADPH, virtually all (97%) of the bound ^{32}P-labeled DNA was present in complex 1.

CbbR induces DNA bending. A number of LysR-type proteins induce a bend in the DNA following binding (31). To investigate whether CbbR bends DNA, the 68-bp *Bam*HI-*Hin*dIII DNA fragment of pSR168 containing the CbbR-binding sites was cloned into pBEND4, yielding pLG168. A series of circular permutated DNA fragments of the same length and differing only in the position of the CbbR-binding sites were isolated following digestion of pLG168 with various enzymes and used in band shift experiments (Fig. 1 and 6A). The results show that the electrophoretic mobility of the DNA-CbbR complex is dependent on the distance between the CbbR-binding sites and the ends of the DNA fragment (Fig. 6C). From the electrophoretic mobilities of the protein-DNA complexes, it was calculated that CbbR introduces a bend α of 64 ± 3° following binding to its cognate binding sites.

NADPH relaxes CbbR-induced DNA bending. It has been reported for some LysR-type proteins that the DNA-bending angle is reduced when the ligand is added to the binding assay (31). To determine whether DNA bending by CbbR is influenced by NADPH, 200 μM NADPH was included in the assay mixture (Fig. 6B and C). Following analysis on nondenaturing gels, a bending angle of 55 ± 3° was calculated, 9° less than that calculated in the absence of NADPH.

DISCUSSION

Physiological studies have shown that the expression of the Calvin cycle in facultatively autotrophic bacteria depends on the availability of suitable carbon and energy sources. The discovery that CbbR is a transcriptional regulator of the *cbb* operons in chemo- and photoautotrophic bacteria (6, 13, 37, 38, 42) suggested that this protein transduces these physiological signals to the transcription apparatus. This paper describes the effects of metabolic intermediates on the in vitro DNA-binding characteristics of purified CbbR.

CbbR of *X. flavus* protects nucleotides −75 and −29 relative to the transcriptional start site of the *cbb* operon. A similar region is protected by CbbR of *Thiobacillus ferrooxidans* and *R. eutropha*, which overlaps the −35 region of the promoter of the *cbb* operon. The close proximity of CbbR-binding sites to the promoter of the *cbb* operon facilitates contact between CbbR and the α subunit of RNA polymerase, which was shown to be important for transcriptional activation by LysR-type regula-
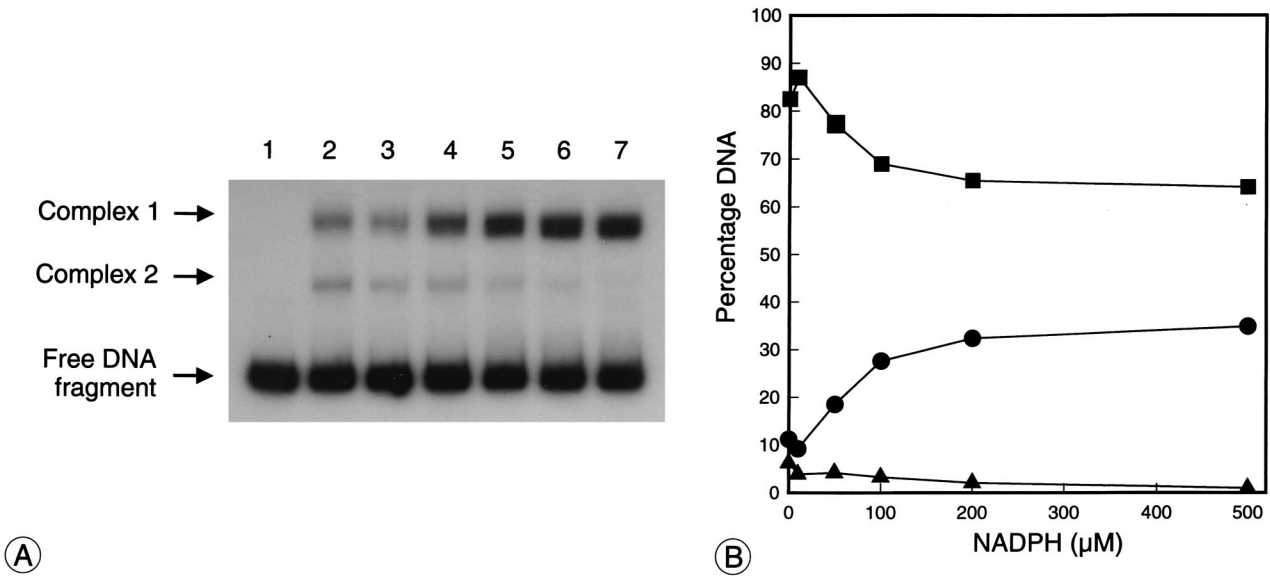
FIG. 5. Effect of NADPH concentration on the DNA-binding characteristics of purified CbbR. (A) Band shift assay using the 277-bp EcoRI-BamHI DNA fragment of pTZ00 and 17 ng of purified CbbR. Lanes: 1, no CbbR added; 2, 0 μM NADPH; 3, 10 μM NADPH; 4, 50 μM NADPH; 5, 100 μM NADPH; 6, 200 μM NADPH; 7,500 μM NADPH. Arrows indicate the positions of the unbound DNA and the protein-DNA complexes of low (complex 1) and high (complex 2) electrophoretic mobility. (B) Graphical representation of the band shift assay results in panel A. The percentages of total ^{32}P-labeled DNA present in protein-DNA complex 1 (●), protein-DNA complex 2 (▲), and the free-DNA fragment (■) are plotted against the NADPH concentration. The amount of ^{32}P-labeled DNA was determined by quantifying the radioactivity in the bands with a PhosphorImager.

tors (8, 35). It has been shown that CbbR of *R. eutropha* acts as a repressor of its own synthesis by binding to the *cbbR* promoter. The DNase I footprint obtained by using CbbR from *X. flavus* shows that this protein binds to the same region as the protein of *R. eutropha*, which overlaps the initiation codon of *cbbR* and upstream sequences (Fig. 1). This strongly indicates

that in *X. flavus*, transcription of the *cbbR* gene is also repressed by CbbR.

DNase I footprinting and band shift assays done by using CbbR of *R. eutropha* showed the presence of two binding sites in the region protected by CbbR from DNase I. The results presented here and in a previous study show that this is also
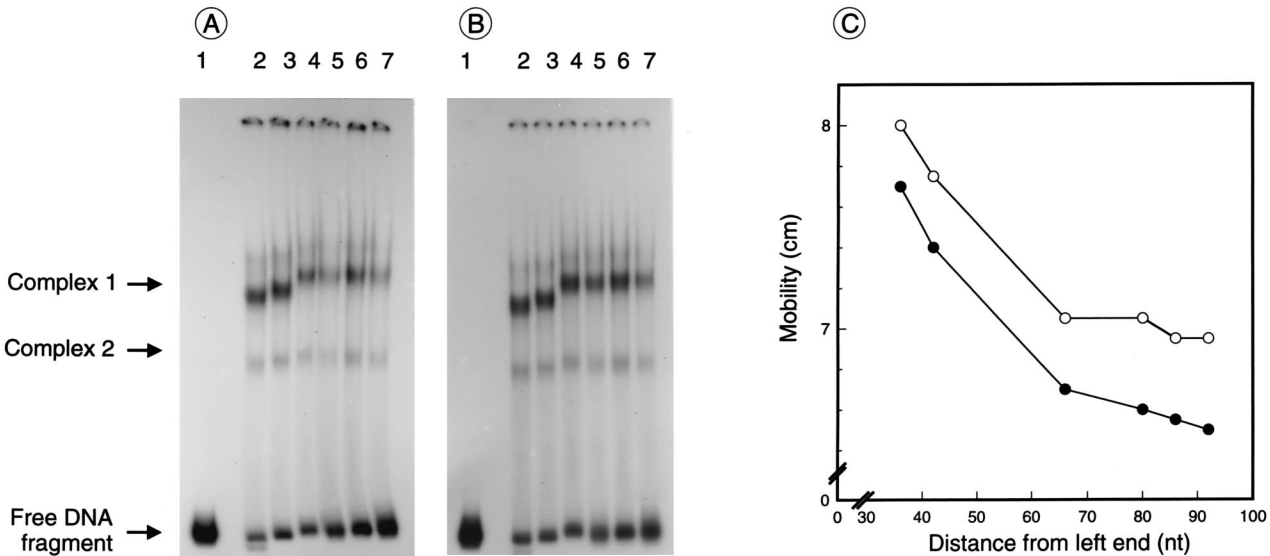

FIG. 6. DNA bending by CbbR in the absence (A) or presence (B) of 200 μM NADPH in the binding assay. Circular permutated DNA fragments of pLG168 containing both CbbR-binding sites were constructed by digestion with various restriction enzymes as described in Materials and Methods. The radiolabeled DNA fragments (10,000 cpm) were incubated with purified CbbR (1.7 μg) and analyzed on a nondenaturing acrylamide gel. Lanes: 1; no CbbR added, *Bgl*II; 2, *Bgl*II; 3, *Nhe*I; 4, *Xho*I; 5, *Eco*RV; 6, *Pvu*II; 7, *Sma*I. (C) Graphical representation of CbbR bending of the *cbbL* promoter region in the absence (●) or presence (○) of 200 μM NADPH, showing electrophoretic mobility (in centimeters) plotted against the position (in nucleotides [nt]) of IR$_1$ and IR$_2$ with respect to the left end of the DNA fragment. The bending angle (α) was calculated as described in Materials and Methods from five experiments.

true for CbbR of *X. flavus* (37). DNA binding by CbbR of both species is therefore typical for LysR-type transcriptional regulators, which, in general, bind to two binding sites upstream from the promoter. Since the region protected by CbbR contains two inverted repeats with a LysR motif, it is likely that these inverted repeats represent CbbR-binding sites.

LysR-type transcriptional regulators use low-molecular-weight compounds as ligands which, upon binding, frequently cause a modest increase or decrease in the DNA-binding affinity of the transcriptional regulator and a decrease in the DNA-bending angle (31). Of all of the metabolites tested, only the addition of NADPH to the binding assay had an effect on the DNA-binding characteristics of CbbR. A classical pyridine dinucleotide binding motif (41) is not present in the primary structure of CbbR. This is not altogether surprising, since binding of NADPH to allosteric sites may be quite different from binding to catalytic sites, which usually display the pyridine dinucleotide binding motif. The addition of NADPH caused a threefold increase in total DNA binding by CbbR. Following the addition of NADPH, 97% of the bound CbbR is present in complex 1, which is formed following the binding of two CbbR dimers to their cognate binding sites. In contrast, only 65% of the total bound CbbR interacts with both sites in the absence of NADPH. CbbR therefore resembles TrpI; binding of TrpI to the promoter-proximal binding site is dependent on the presence of the ligand indoleglycerol phosphate (3). Interestingly, CbbR from *R. eutropha* resembles NodD in that binding to both binding sites is independent of the protein concentration and the presence of a ligand. The CbbR proteins of *R. eutropha* and *X. flavus* therefore display different DNA-binding characteristics, although both bind to two binding sites.

CbbR from *X. flavus* induces DNA bending, which is relaxed in the presence of NADPH. The presence of DNase I-hypersensitive sites between the two CbbR-binding sites in a footprint of the *cbb* promoter of *R. eutropha* suggests that CbbR of this bacterium also bends its target DNA (14). It has been shown that DNA bending strongly influences the activity of some promoters (27). This may be due to a conformational change in the DNA helix or, alternatively, may facilitate the formation of productive contacts with RNA polymerase. DNA bending and ligand-induced relaxation of the DNA bend were observed in studies on other LysR-type proteins (31). In OxyR and OccR, relaxation of the DNA bend is associated with repositioning of the LysR-type regulator in the promoter-proximal DNA-binding site (36, 39).

The results of the in vitro experiments described here strongly suggest, but do not prove, that in vivo transcriptional regulation of the *cbb* and *gap-pgk* operons by CbbR is regulated by the intracellular concentration of NADPH. A number of experiments show that autotrophic growth is associated with elevated levels of NADPH. The transition of *P. oxalaticus* from heterotrophic to autotrophic growth is accompanied by an increase in the intracellular NADPH-to-NADP ratio (12). Furthermore, NADP is completely reduced during incubation of *Rhodospirillum rubrum* under anaerobic conditions in the light. NADPH was rapidly oxidized following exposure to oxygen or in the dark. Interestingly, *R. rubrum* induces the Calvin cycle under the former growth conditions but not under the latter two (11).

Although bacteria use NADH to drive assimilation of CO_2 by the Calvin cycle, NADPH may be a better signal in the regulation of Calvin cycle gene expression. NADPH, produced from NADH by transhydrogenase, is used in biosynthesis. A high intracellular NADPH concentration may therefore signal that although sufficient reducing power is available, biosynthetic reactions do not proceed due to the lack of a source of carbon. This is alleviated by the addition of suitable carbon sources to the medium or by induction of the Calvin cycle, followed by the fixation of CO_2. The regulation of the *cbb* operon by the intracellular concentration of NADPH therefore explains why the oxidation of unrelated compounds such as thiosulfate, molecular hydrogen, and methanol induces expression of the Calvin cycle, whereas virtually all carbon sources which are readily assimilated have a repressive effect.

The present study strongly suggests that NADPH plays an important role in the transcriptional regulation of the Calvin cycle genes. Future research will aim to characterize the in vivo and in vitro transcriptional regulation of the *cbb* and *gap-pgk* operons by the intracellular concentration of NADPH and the interaction between CbbR and NADPH.

REFERENCES

1. **Birnboim, H. C., and J. Doly.** 1979. A rapid alkaline extraction procedure for screening recombinant plasmid DNA. Nucleic Acids Res. **7:**1513–1523.
2. **Bradford, M. M.** 1976. A rapid and sensitive method for the quantitation of microgram quantities of protein utilizing the principle of protein-dye binding. Anal. Biochem. **73:**248–254.
3. **Chang, M., and I. P. Crawford.** 1990. The roles of indoleglycerol phosphate and the TrpI protein in the expression of *trpBA* from *Pseudomonas aeruginosa*. Nucleic Acids Res. **18:**979–988.
4. **Croes, L. M., W. G. Meijer, and L. Dijkhuizen.** 1991. Regulation of methanol oxidation and carbon dioxide fixation in *Xanthobacter* strain 25a grown in continuous culture. Arch. Microbiol. **155:**159–163.
5. **Falcone, D. L., and F. R. Tabita.** 1993. Complementation analysis and regulation of CO_2 fixation gene expression in a ribulose 1,5-bisphosphate carboxylase-oxygenase deletion strain of *Rhodospirillum rubrum*. J. Bacteriol. **175:**5066–5077.
6. **Gibson, J. L., and F. R. Tabita.** 1993. Nucleotide sequence and functional analysis of CbbR, a positive regulator of the Calvin cycle operons of *Rhodobacter sphaeroides*. J. Bacteriol. **175:**5778–5784.
7. **Goethals, K., M. van Montagu, and M. Holsters.** 1992. Conserved motifs in a divergent *nod* box of *Azorhizobium caulinodans* ORS571 reveal a common structure in promoters regulated by LysR-type proteins. Proc. Natl. Acad. Sci. USA **89:**1646–1650.
8. **Gussin, G. N., C. Olson, K. Igarashi, and A. Ishihama.** 1992. Activation defects caused by mutations in *Escherichia coli rpoA* are promoter specific. J. Bacteriol. **174:**5156–5160.
9. **Hallenbeck, P. L., R. Lerchen, P. Hessler, and S. Kaplan.** 1990. Roles of CfxA, CfxB, and external electron acceptors in regulation of ribulose-1,5-bisphosphate carboxylase/oxygenase expression in *Rhodobacter sphaeroides*. J. Bacteriol. **172:**1736–1748.
10. **Im, D.-S., and C. G. Friedrich.** 1983. Fluoride, hydrogen, and formate activate ribulosebisphosphate carboxylase formation in *Alcaligenes eutrophus*. J. Bacteriol. **154:**803–808.
11. **Jackson, J. B., and A. R. Crofts.** 1968. Energy-linked reduction of nicotinamide adenine dinucleotides in cells of *Rhodospirillum rubrum*. Biochem. Biophys. Res. Commun. **32:**908–915.
12. **Knight, M., L. Dijkhuizen, and W. Harder.** 1978. Metabolic regulation in *Pseudomonas oxalaticus* OX1. Enzyme and coenzyme concentration changes during substrate transition experiments. Arch. Microbiol. **116:**85–90.
13. **Kusano, T., and K. Sugawara.** 1993. Specific binding of *Thiobacillus ferrooxidans* RbcR to the intergenic sequence between the *rbc* operon and the *rbcR* gene. J. Bacteriol. **175:**1019–1025.
14. **Kusian, B., and B. Bowien.** 1995. Operator binding of the CbbR protein, which activates the duplicate *cbb* CO_2 assimilation operons of *Alcaligenes eutrophus*. J. Bacteriol. **177:**6568–6574.
15. **Lascelles, J.** 1960. The formation of ribulose 1:5-diphosphate carboxylase by growing cultures of Athiorhodaceae. J. Gen. Microbiol. **23:**499–510.
16. **Lehmicke, L. G., and M. E. Lidstrom.** 1985. Organization of genes necessary for growth of the hydrogen-methanol autotroph *Xanthobacter* sp. strain H4-14 on hydrogen and carbon dioxide. J. Bacteriol. **162:**1244–1249.
17. **Lidstrom-O'Conner, M. E., G. L. Fulton, and A. E. Wopat.** 1983. 'Methylobacterium methanolicum': a syntrophic association of two methylotrophic bacteria. J. Gen. Microbiol. **129:**3139–3148.
18. **Meijer, W. G.** 1994. The Calvin cycle enzyme phosphoglycerate kinase of *Xanthobacter flavus* required for autotrophic CO_2 fixation is not encoded by the *cbb* operon. J. Bacteriol. **176:**6120–6126.
19. **Meijer, W. G., A. C. Arnberg, H. G. Enequist, P. Terpstra, M. E. Lidstrom,**

and L. Dijkhuizen. 1991. Identification and organization of carbon dioxide fixation genes in *Xanthobacter flavus* H4-14. Mol. Gen. Genet. **225:**320–330.

20. **Meijer, W. G., L. M. Croes, B. Jenni, L. G. Lehmicke, M. E. Lidstrom, and L. Dijkhuizen.** 1990. Characterization of *Xanthobacter* strains H4-14 and 25a and enzyme profiles after growth under autotrophic and heterotrophic growth conditions. Arch. Microbiol. **153:**360–367.

21. **Meijer, W. G., P. de Boer, and G. van Keulen.** 1997. *Xanthobacter flavus* employs a single triosephosphate isomerase for heterotrophic and autotrophic metabolism. Microbiology **143:**1925–1931.

22. **Meijer, W. G., and L. Dijkhuizen.** 1988. Regulation of autotrophic metabolism in *Pseudomonas oxalaticus* OX1 wild-type and an isocitrate-lyase-deficient mutant. J. Gen. Microbiol. **134:**3231–3237.

23. **Meijer, W. G., H. G. Enequist, P. Terpstra, and L. Dijkhuizen.** 1990. Nucleotide sequences of the genes encoding fructosebisphosphatase and phosphoribulokinase from *Xanthobacter flavus* H4-14. J. Gen. Microbiol. **136:** 2225–2230.

24. **Meijer, W. G., E. R. E. van den Bergh, and L. M. Smith.** 1996. Induction of the *gap-pgk* operon encoding glyceraldehyde-3-phosphate dehydrogenase and 3-phosphoglycerate kinase of *Xanthobacter flavus* requires the LysR-type transcriptional activator CbbR. J. Bacteriol. **178:**881–887.

25. **Paoli, G. C., N. S. Morgan, F. R. Tabita, and J. M. Shively.** 1995. Expression of the *cbbLcbbS* and *cbbM* genes and distinct organization of the *cbb* Calvin cycle structural genes of *Rhodobacter capsulatus*. Arch. Microbiol. **164:**396–405.

26. **Papavassiliou, A. G.** 1994. 1,10-Phenanthroline-copper ion nuclease footprinting of DNA-protein complexes *in situ* following mobility shift electrophoresis assays. Methods Mol. Biol. **30:**43–78.

27. **Pérez-Martín, J., F. Rojo, and V. de Lorenzo.** 1994. Promoters responsive to DNA bending: a common theme in procaryotic gene expression. Microbiol. Rev. **58:**268–290.

28. **Reutz, I., P. Schobert, and B. Bowien.** 1982. Effect of phosphoglycerate mutase deficiency on heterotrophic and autotrophic carbon metabolism of *Alcaligenes eutrophus*. J. Bacteriol. **151:**8–15.

29. **Richardson, D. J., G. F. King, D. J. Kelly, A. G. McEwan, S. J. Ferguson, and J. B. Jackson.** 1988. The role of auxiliary oxidants in maintaining the redox balance during phototrophic growth of *Rhodobacter capsulatus* on propionate or butyrate. Arch. Microbiol. **150:**131–137.

30. **Sambrook, J., E. F. Fritsch, and T. Maniatis.** 1989. Molecular cloning: a laboratory manual, 2nd ed. Cold Spring Harbor Laboratory Press, Cold Spring Harbor, N.Y.

31. **Schell, M. A.** 1993. Molecular biology of the LysR family of transcriptional regulators. Annu. Rev. Microbiol. **47:**597–626.

32. **Strecker, M., E. Sickinger, R. S. English, J. M. Shively, and E. Bock.** 1994. Calvin cycle genes in *Nitrobacter vulgaris* T3. FEMS Microbiol. Lett. **120:**45–50.

33. **Studier, F. W., A. H. Rosenberg, J. J. Dunn, and H. J. W. Dubendorf.** 1990. Use of T7 RNA polymerase to direct expression of cloned genes. Methods Enzymol. **185:**60–89.

34. **Tabita, F. R.** 1988. Molecular and cellular regulation of autotrophic carbon dioxide fixation in microorganisms. Microbiol. Rev. **52:**155–189.

35. **Tao, K., C. Zou, N. Fujita, and A. Ishihama.** 1995. Mapping of the OxyR protein contact site in the C-terminal region of RNA polymerase α subunit. J. Bacteriol. **177:**6740–6744.

36. **Toledano, M. B., I. Kullik, F. Trinh, P. T. Baird, T. D. Schneider, and G. Storz.** 1994. Redox-dependent shift of OxyR-DNA contacts along an extended DNA-binding site: a mechanism for differential promoter selection. Cell **78:**897–909.

37. **van den Bergh, E. R. E., L. Dijkhuizen, and W. G. Meijer.** 1993. CbbR, a LysR-type transcriptional activator, is required for expression of the autotrophic CO₂ fixation enzymes of *Xanthobacter flavus*. J. Bacteriol. **175:**6097–6104.

38. **Viale, A. M., H. Kobayashi, T. Akazawa, and S. Henikoff.** 1991. *rbcR*, a gene coding for a member of the LysR family of transcriptional regulators, is located upstream of the expressed set of ribulose 1,5-bisphosphate carboxylase/oxygenase genes in the photosynthetic bacterium *Chromatium vinosum*. J. Bacteriol. **173:**5224–5229.

39. **Wang, L., and S. C. Winans.** 1995. High angle and ligand-induced low angle DNA bends incited by OccR lie in the same plane with OccR bound to the interior angle. J. Mol. Biol. **253:**32–38.

40. **Wang, X., D. L. Falcone, and F. R. Tabita.** 1993. Reductive pentose phosphate-independent CO₂ fixation in *Rhodobacter sphaeroides* and evidence that ribulose bisphosphate carboxylase/oxygenase activity serves to maintain the redox balance of the cell. J. Bacteriol. **175:**3372–3379.

41. **Wieringa, R. K., P. Terpstra, and W. G. J. Hol.** 1986. Prediction of the occurrence of the ADP-binding βαβ-fold in proteins, using an amino acid sequence fingerprint. J. Mol. Biol. **187:**101–107.

42. **Windhövel, U., and B. Bowien.** 1991. Identification of *cfxR*, an activator gene of autotrophic CO₂ fixation in *Alcaligenes eutrophus*. Mol. Microbiol. **5:**2695–2705.

43. **Zwieb, C., and S. Adhya.** 1994. Improved plasmid vectors for the analysis of protein-induced DNA bending. Methods Mol. Biol. **30:**281–294.